Monte Carlo Simulation of Electron Transport in InSb

Ömer ÖZBAŞ, Mustafa AKARSU
Osmangazi University, Physics Department, 26480, Eskişehir-TURKEY
e-mail: oozbas@ogu.edu.tr, makarsu@ogu.edu.tr

Abstract

Transport properties of indium antimonide in an electric field have been calculated at 77 K. The calculation shows that ionized impurity scattering plays a dominant role in InSb at low electric field. The mobility, mean energy, and drift velocity are calculated as a function of the electric field strength, and comparison is made with previous theoretical results. Types of the scattering mechanisms and percentage of each mechanism in the total scattering events are determined.

Key Words: Transport properties; Scattering rates; Infrared dedectors; Monte Carlo.

1. Introduction

The problems of high-field transport in semiconductors have been extensively investigated both theoretically and experimentally for many years. Many numerical methods available in the literature (Monte Carlo method, Iterative method, Variational method, Relaxation time approximation, or Matthiessen's rule) have lead to approximate solutions to the Boltzmann transport equation. The Monte Carlo method has been widely used to study hot-electron problems. The principle of this method is to simulate on a computer the motion of one electron in momentum space through a large number of scattering processes taking note of the time that the electron spends in each element of momentum space during its flight, this times being proportional to the distribution function in the elements. The procedure used for following the motion of an electron requires random numbers to represent the time which the electron drifts before being scattered, and to represent the final state after the scattering event. The probability distribution for these random numbers can be completely specified in terms of the electric field strength and the transition probabilities due to the various scattering processes [1].

Study on the InSb has been concentrated on producing high quality material for application in infrared detection [2]. InSb, with the smallest band gap of III-V binary semiconductors, has the lightest electron effective mass and the highest electron mobility. The scattering mechanisms, which limit the low field electron drift velocity in InSb, are ionized impurity scattering, significant at low temperatures; and polar mode optical phonon scattering dominant at room temperatures. Intervalley scattering is negligible in InSb, the $\Gamma - L$ and $\Gamma - X$ intervalley separations being of the order of 1 eV [3].

The electron drift velocity in InSb increases nonlinearly under the influence of high electric field to a peak value at a threshold field, after which any further increase of electric field results in reduced drift velocity, giving rise to a negative differential resistance. In this work, we study velocity-field characteristics of InSb.

2. The Band Structure and Scattering Mechanisms in Indium Antimonide

InSb is a direct semiconductor. The minimum of the conduction band is situated in the center of the Brillouin zone. Near the minimum, $E(k)$ is isotropic but non-parabolic [4]. For values of $\vec{k}$ far from the minima of the conduction band, the energy deviates from the simple quadratic expressions and nonparabolicity occurs. We shall assume that the valley is spherical at all energies of interest; thus to take into account the nonparabolicity is to consider an energy-wave vector relation of the type (Conwell and Vassel, 1968) [5].

$$\frac{\hbar^2 k^2}{2m} = \gamma(E) = E(1 + \alpha E) \tag{1}$$

$$\alpha = \frac{1}{E_g}\left(1 - \frac{m*}{m_0}\right)^2, \tag{2}$$

where $m*$ and m_0 are the effective electron mass at the bottom of the band and the free electron mass, respectively, and E_g is the energy gap of semiconductor.

The scattering rate due to the polar optical phonon is given by [6]:

$$\lambda_o(k) = \frac{em*^{1/2} w_0}{\sqrt{2}\hbar}\left(\frac{1}{\varepsilon_\infty} - \frac{1}{\varepsilon_0}\right)\frac{(1 + 2\alpha E')}{\gamma^{1/2}(E)}F_o(E, E') \times \left\{\begin{array}{ll} N_0 & \text{(absorption)} \\ (N_0 + 1) & \text{(emission)} \end{array}\right\} \tag{3}$$

where

$$E' = \left\{\begin{array}{ll} E + \hbar w_0 & \text{(absorption)} \\ E - \hbar w_0 & \text{(emission)} \end{array}\right\}$$

and

$$F_0(E, E') = C^{-1}\left(A\ \ln\left|\frac{\gamma^{1/2}(E) + \gamma^{1/2}(E')}{\gamma^{1/2}(E) - \gamma^{1/2}(E')}\right| + B\right)$$

$$A = [2(1 + \alpha E)(1 + \alpha E') + \alpha\{\gamma(E) + \gamma(E')\}]^2$$

$$B = -2\alpha\gamma^{1/2}(E)\gamma^{1/2}(E')[4(1 + \alpha E)(1 + \alpha E') + \alpha\{\gamma(E) + \gamma(E')\}]$$

$$C = 4(1 + \alpha E)(1 + \alpha E')(1 + 2\alpha E)(1 + 2\alpha E')$$

$$N_0 = [\exp(\hbar w_0/k_B T_L) - 1]^{-1}.$$

$\gamma(E)$ is defined by Equation (1), and w_0 is the optical-phonon frequency. N_0 is the polar optical phonon occupation number, and T_L is the lattice temperature. For high-energy electrons, the scattering rate is not strongly dependent on the electron energy. It should also be noted that a threshold energy $\hbar w_0$ exists for the phonon emission process. The magnitude of the scattering rate for the phonon emission process is several times larger than that for the phonon absorption process.

Vibrations of the ions about their equilibrium positions produce instantaneous change of the energy band and thus cause the scattering of electrons. For a small change in the lattice constant, a small change in the energy band can be expected. This may be considered proportional to the change in lattice spacing and can be expressed by the induced strain $\vec{\nabla} \cdot \vec{U}(\vec{r}, t)$. The lattice spacing change is not expressed by the displacement $\vec{U}(\vec{r}, t)$ alone. Thus, we write the interaction potential for acoustic phonons as

$$H' = \Xi_d \vec{\nabla} \cdot \vec{U}(\vec{r}, t),$$

where the proportionality constant Ξ_d is called the deformation potential. $\vec{\nabla} \cdot \vec{U}$ vanishes for transverse phonons, therefore the deformation potential applies only to longitudinal phonons.

The scattering rate for the acoustic phonon scattering is given by [6]:

$$\lambda_a(k) = \frac{(2m*)^{3/2} k_B T_L \Xi_d^2}{2\pi \rho s^2 \hbar^4} \gamma^{1/2}(E)(1 + 2\alpha E) F_a(E), \tag{4}$$

where

$$F_a(E) = \frac{(1 + \alpha E)^2 + \frac{1}{3}(\alpha E)^2}{(1 + 2\alpha E)^2},$$

ρ is the density of the material and s is the velocity of longitudinal elastic waves. The acoustic phonon scattering rate increases with the increase of the electron energy because it depends on the density of states that increases with electron energy.

Carriers are scattered when they encounter the electric field of an ionized impurity. The potential due to an impurity charge in a crystal is screened depending on how many free carriers are present. The scattering rate due to the ionized impurity scattering is [7]

$$\lambda_i(k) = \frac{2\sqrt{2}\pi n e^4 m*^{1/2}}{\varepsilon_0^2 \hbar^2 \beta^2} \frac{(1 + 2\alpha E)}{[E(1 + \alpha E)]^{1/2}}, \tag{5}$$

where β is the inverse of screening length and is related to the electron concentration n by

$$\beta^2 = \frac{4\pi n e^2}{\varepsilon_0 k_B T_L}.$$

3. Results and Discussion

The parameters used in the calculations, shown in Table 1, have been taken from [8-11]. The fundamental material parameters and the Γ valley effective mass have been taken from Madelung [4].

There are some values of Ξ_d reported in the literature 7.2 and 30 eV [8]. When we take the value of 30 eV for the acoustic deformation potential, we find better agreement with reported experimental values of electron drift velocity and mobility. Therefore, we have carried out our calculations by taking Ξ_d=30 eV.

Table 1. Parameters used in present calculations (extracted from [8-11]).

| Parameter	Value	Parameter	Value
Effective mass ratio (m*/m$_o$)	0.014	Acoustic deformation potential (eV)	30.0
Lattice temperature (K)	77	Energy gap (eV)	0.24
Electron concentration(cm^{-3})	1x10^{15}	Static dielectric constant (ε_0)	17.9
Density (g/cm^3)	5.79	High-frequency dielectric constant (ε_∞)	15.7
Velocity of sound (cm/s)	3.7x10^5	Optical phonon energy (meV)	25.0

In Figure 1 electron drift velocity versus electric field characteristics obtained from Monte Carlo calculations with the parameters in Table 1 are shown. In order to discuss this curve let us first point out that energy equilibrium is maintained at low fields mainly by ionized impurity scatterings. Ionized impurity scattering events during the simulation time decrease quickly with the increasing electric field strength up to 300 V/cm while polar optical phonon scatterings increase clearly and acoustic phonon scattering events nearly zero. At this field strength 75% of the total scattering events occurring in the simulation time of 2 ns are due to ionized impurity and nearly 25% of the total scattering event is polar optical phonon scattering, as shown in Figure 3. However, total scattering events occurring in the simulation time decrease clearly with the increasing electric field strength up to 400 V/cm. Since the total scattering events decrease, electrons are more effectively accelerated and, as a result mean drift velocity achieves 4.5×10^7 cm/s, maximum value in our simulation at 400 V/cm. It is reported in Asauskas [12] as 4×10^7 cm/s and in Fawcett [10] as 5.5×10^7 cm/s for InSb at 77 K. Figure 2. shows the mean energy of the electrons in the central valley as a function of field strength. From the analysis of Figure 2 it is possible to verify that the above description does represent the physical situation. Mean electron energy increases slowly at first from the zero field to 200 V/cm. Beyond the field of 200 V/cm, ionized impurity scattering number continues to decrease to 700 V/cm and polar optical phonon scattering number continues to increase to about 400 V/cm. At this field mean elec-
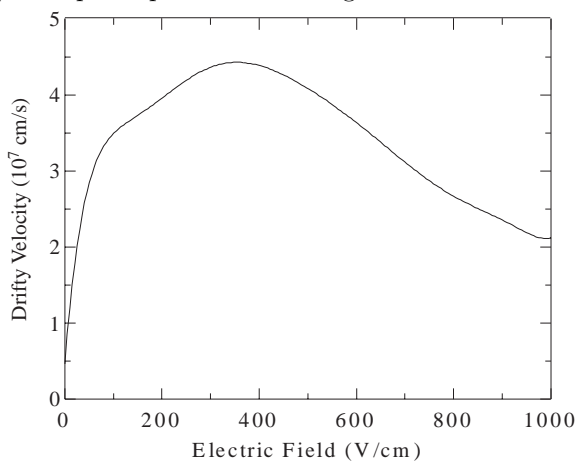

Figure 1. Drift velocity of electrons as a function of the field strenght at 77 K.
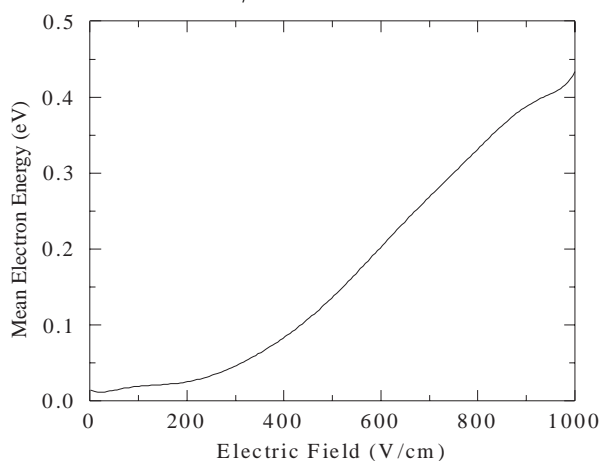
Figure 2. Mean electron energy in the central valley as a function of the applied electric field at 77 K.
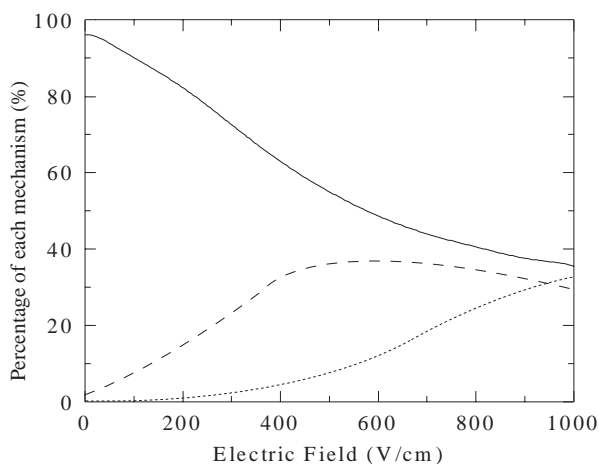

Figure 3. Percentage of each mechanism in total scattering events in 2 ns as a function of the electric field. Dotted line is due to the polar optical phonon, dashed line is due to the the acoustic phonon, and solid line is due to the ionized impurity scattering contributions.
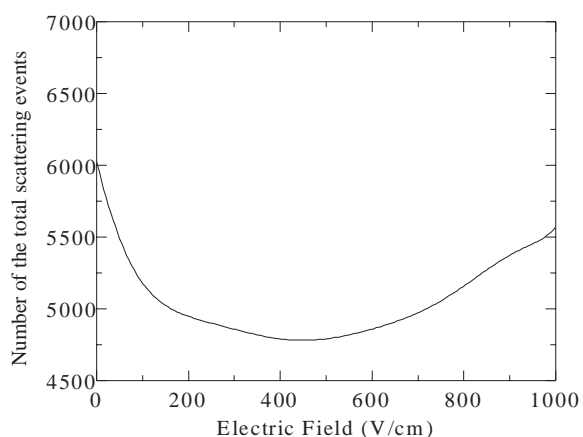
Figure 4. Number of the total scattering events occuring in the simulation time of 2 ns as a function of the electric field.

tron energy achieves 0.08 eV and acoustic phonon scattering mechanism starts to increase slowly. Therefore, the number of total scattering events increases, starting at this field strength, as shown in Figure 4. As a result electron drift velocity decreases beginning from 400 V/cm.

In Figure 5 we show the calculated results for the electric field dependence of the mobility in the central valley at 77 K. The low field mobility is calculated to be about 1.15×10^7 cm^2/Vs , whereas it is reported in Fawcett [10] as 1.7×10^6 cm^2/Vs and experimentally in Chin [3] as 2×10^6 cm^2/Vs. When we take the value of 7.2 eV instead of 30 eV for the acoustic deformation potential, we find the low field mobility to be about 1.6×10^7 cm^2/Vs.
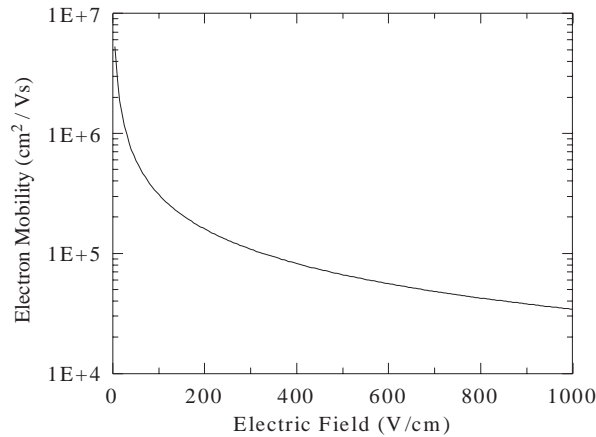
Figure 5. Electric field dependence of the mobility at 77 K.

In conclusion, effects of the scattering mechanisms on the drift velocity, the mean electron energy and the low field mobility of InSb are determined. Our calculations indicate that the drift velocity and the low field mobility are limited by strongly ionized impurity scatterings. Our results for the drift velocity and the low field mobility are in reasonable agreement with the reported data.

References

[1] C. Jacoboni and P. Lugli, *The Monte Carlo Method for Semiconductor Device Simulation,* (Springer-Verlag, New York,1989) p. 104.

[2] V. W. L. Chin, R. J. Egan, and T. L. Tansley, *J. Appl. Phys.,* **69** (6), (1991), 3571.

[3] V W. L. Chin, R. J. Egan, and T. L. Tansley, *J. Appl. Phys.*, **72** (4), (1992), 1410.

[4] Otfried Madelung, *Semiconductors-Basic Data,* (Springer-Verlag, New York,1986) p. 141.

[5] Carlo Jacoboni and Lino Reggiani, *Rev. Mod. Phys.*, **55** (3), (1983), 645.

[6] W. Fawcett, A. D. Boardman, and S. Swain, *J. Phys. Chem. Solids.*, **31**, (1970), 1963.

[7] J. G. Ruch and W. Fawcett, *J. Appl. Phys.*, **41**(9), (1970), 3843.

[8] B. R. Nag and G. M. Dutta, *Phys. Stat. Sol. (b).*,**71**, (1975), 401.

[9] S. S. Paul, A. K. Ghorai, D. P. Bhattacharya, *Physica B.*, **212**, (1995), 158.

[10] W. Fawcett and J. G. Ruch, *Appl. Phys. Lett.,* **15 (**11), (1969), 368.

[11] B. R. Nag, *J. Appl. Phys.*, **44** (4), (1973), 1888.

[12] Asauskas, R., Z. Dobrovolskis, and A. Krotkus, *Sov. Phys. Semicond.*, **14** (12), (1980), 1377.